Hybrid nanostructures for efficient light harvesting

2010 J. Phys.: Condens. Matter 22 193102

(http://iopscience.iop.org/0953-8984/22/19/193102)

IOP Publishing Journal of Physics: Condensed Matter

J. Phys.: Condens. Matter **22** (2010) 193102 (17pp) doi:10.1088/0953-8984/22/19/193102

TOPICAL REVIEW

Hybrid nanostructures for efficient light harvesting

Sebastian Mackowski[1]

Optics of Hybrid Nanostructures Group, Institute of Physics, Nicolaus Copernicus University, Grudziadzka 5/7, 87-100 Torun, Poland

E-mail: mackowski@fizyka.umk.pl

Received 26 January 2010, in final form 16 March 2010
Published 23 April 2010
Online at stacks.iop.org/JPhysCM/22/193102

Abstract

Hybrid nanostructures are systems composed of two or more nanostructures designed for improving the performance over individual components. In this work we introduce the concept of bridging natural photosynthetic protein–pigment complexes with nanostructures fabricated in an artificial way, such as semiconductor nanocrystals, metallic nanoparticles or carbon nanotubes, with the purpose of enhancing the efficiency of light harvesting either via plasmon excitation in metals or absorption tunability characteristics of semiconductors. In addition to presenting basic features of inorganic nanostructures, we discuss recent advances in the field of hybrid nanostructures composed of photosynthetic pigment–protein complexes.

(Some figures in this article are in colour only in the electronic version)

Contents

[1] welcome.fizyka.umk.pl

1. Introduction

One of the most attractive sources of alternative energy is solar energy. It is enough to realize that during one minute more solar energy hits the surface of the Earth than the whole human population consumes over a year [1]. The ability to collect even a few per cent of this energy and efficiently transform it into some form of usable energy would provide a very attractive and perhaps complete solution for our ever-growing energy needs. Our present understanding of the structure and function of how photosynthetic organisms convert sunlight energy into chemical energy has opened possibilities to explore ways to develop novel solar energy devices, either by mimicking biology [2, 3], or employing biological systems in hybrid devices [4, 5]. These efforts have been helped by enormous progress in determining the structures of the proteins involved in photosynthesis using x-ray crystallography. At present many of them are known with an accuracy better than 5 Å, including exact locations and orientations of pigments as well as their binding within the protein scaffolds. This knowledge is of paramount importance for precise and correct interpretation of spectroscopic data obtained on these structures. Since many of the processes, especially at the primary stage of photosynthesis, such as light harvesting and charge separation,

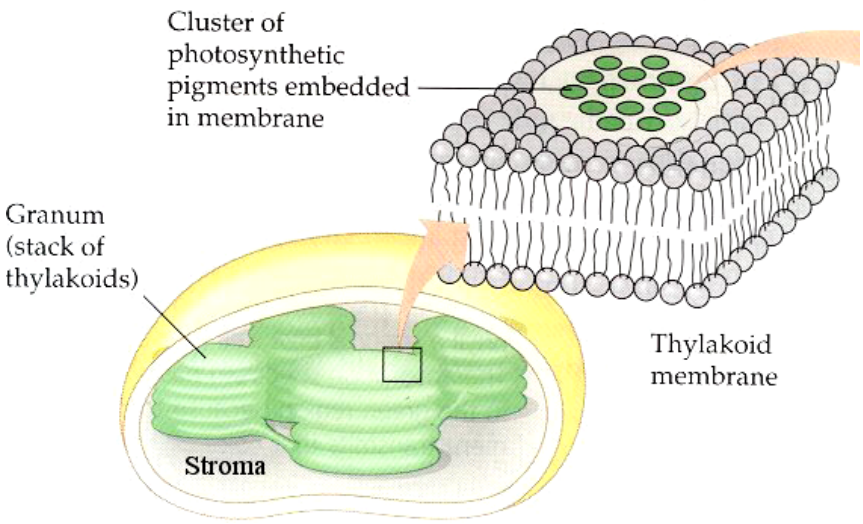

Figure 1. Picture of a chloroplast (courtesy of Dr Trevor Gallant).

are carried out by protein complexes with sizes below 100 nm, assembling them into hybrid devices require control and agile manipulation of structures on the nanoscale level as well as designing ways to probe interactions within such small constructs. These possibilities have been opened up by chemical synthesis of nanostructures and their biochemical conjugation as well as the continuous development of tools used by nanotechnology. In this paper we describe several recent experiments focused on applying nanotechnology towards designing novel hybrid nanostructures comprising biological photosynthetic systems and nanostructures that can be synthesized in the laboratory. These could be semiconductor nanocrystals, metallic nanoparticles or carbon nanotubes. Such hybrid systems, through combining the properties of the constituents, provide a novel paradigm for designing photovoltaic devices.

The main purpose of this subjective review is to outline the enormous potential in combining systems of various structures and functionalities in order to exploit their unique properties for devising strategies of more efficient harnessing of solar energy. It is organized as follows: first, brief characteristics of photosynthesis will be given together with a description of several photosynthetic complexes. This will be followed with an overview of the optical properties of semiconductor and metal nanoparticles. Exemplary experiments showing the potential of hybrid nanostructures for harvesting sunlight will be discussed next. It is important to realize that research in this field has been initiated relatively recently, as it required both an understanding of the structure and function of photosynthetic protein complexes as well as a high degree of manipulation of matter on the nanoscale. Nevertheless, the progress have been considerable and with many new proposals and approaches appearing every year it should be possible to 'improve on Nature' and design a hybrid system with enhanced response to sunlight for efficient conversion of solar energy.

2. Photosynthesis

The energy of the Sun is the source of life on Earth. Billions of years ago, long before any green plants appeared on our planet, certain cyanobacteria had developed the photosynthesis process in order to drive their life processes. Since then evolution has been optimizing strategies to harvest sunlight energy and convert it into chemical energy. As a result, many forms of a highly efficient photosynthesis apparatus found in various organisms like green plants, bacteria and algae have been developed [6]. Photosynthetic organisms are divided between two groups. When photosynthesis is carried out in the presence of air, as for plants, algae and cyanobacteria, it is called oxygenic photosynthesis, which concerns the reduction of carbon dioxide to carbohydrate and oxidation of water to produce molecular oxygen. In the case of anoxygenic photosynthesis, carried out, for instance, by purple bacteria, molecules other than water are subject to oxidation. In this process no oxygen is released. Regardless of these differences, the general principles of energy transduction are the same in anoxygenic and oxygenic photosynthesis.

Although the chemical reaction describing photosynthesis looks relatively simple ($6H_2O + 6CO_2 \rightarrow C_6H_{12}O_6 + 6O_2$), it requires a vast and complex machinery located in that part of cells called chloroplasts [1]. A typical plant cell contains about 10 to 100 chloroplasts. The chloroplasts, in turn, include phospholipid outer and inner membranes as well as an intermembrane space between them, as displayed in figure 1. Within the membrane is an aqueous fluid called the stroma which contains thylakoids. Thylakoids are plate-like structures stacked together, which significantly increases the effective area of the photosynthetic apparatus. They bind photosystems, i.e. protein complexes containing chlorophyll, the major photosynthetic pigment. Therefore, thylakoids are the basic structural units of the cell where photosynthesis takes place.

The whole photosynthesis process can be divided into two phases: the light reaction followed by the dark reaction. In

the first phase, which takes place in the thylakoid membrane, light is absorbed by chlorophylls and other pigments present in photosystems. This energy is then converted into chemical energy stored in the form of adenosine triphosphate (ATP) and reduced nicotine adenine dinucleotide phosphate (NADPH). Water is split in the process, releasing oxygen as a by-product of the reaction. The dark reaction, which uses the products of the light reaction, ATP and NADPH, takes place in the stroma within the chloroplast and converts CO_2 to sugar. This phase involves a cycle called the Calvin cycle in which CO_2 and energy from ATP are used to form sugar.

3. Photosynthetic protein complexes

Protein complexes that participate in photosynthesis can be divided into two groups: complexes containing reaction centers which carry out charge separation and complexes responsible solely for harvesting the sunlight and transferring it to the reaction centers. Large proteins of Photosystem I and Photosystem II fall into the first category, while light-harvesting complex 2 (LH2) from purple bacteria and the peridinin–chlorophyll–protein complex from algae belong to the second group. The description of the structures as well as the presentation of selected optical properties of these pigment–protein systems is vital when discussing their applicability for hybrid nanoscale devices.

3.1. Photosystems

The primary processes of the light reaction are carried out by pigment–protein complexes called photosystems: photosystem I (PS I) and photosystem II (PS II). They are responsible for the absorption of photons, efficient transfer of excitation energy and the primary charge separation across the photosynthetic membrane. The main absorption bands of PS I and PS II are located in the red spectral region, around 700 nm and 680 nm, respectively. In order to increase the spectral range of the light absorbed by the photosynthetic organisms and the effective cross section for capturing a photon, many light-harvesting complexes have evolved, with absorption maxima extending from the blue to red spectral region, thus covering all visible light spectrum. The charge separation takes place in the center of the photosystem, called a reaction center (RC), which is also a pigment–protein complex. The RC absorbs infrared light (from 870 nm to 960 nm, depending on the species) and is a final acceptor of the energy harvested by the light-harvesting complexes. This energy is used to promote pigments located within the RC to the excited state and trigger a chain process that results in electron and proton extraction from the RC. These charges are used for the next stages of photosynthesis.

The crystallographic structures of photosystem I (PS I) and photosystem II (PS II), the two membrane pigment–protein complexes taking part in oxygenic photosynthesis, are shown in figure 2. The brown color represent the protein while green shows the Chl *a* molecules. The PS I complex [7] in its native form is a trimer with each of the monomers containing 96 molecules of Chl *a*, two of which form a special pair in the reaction center, with the other four closely associated with

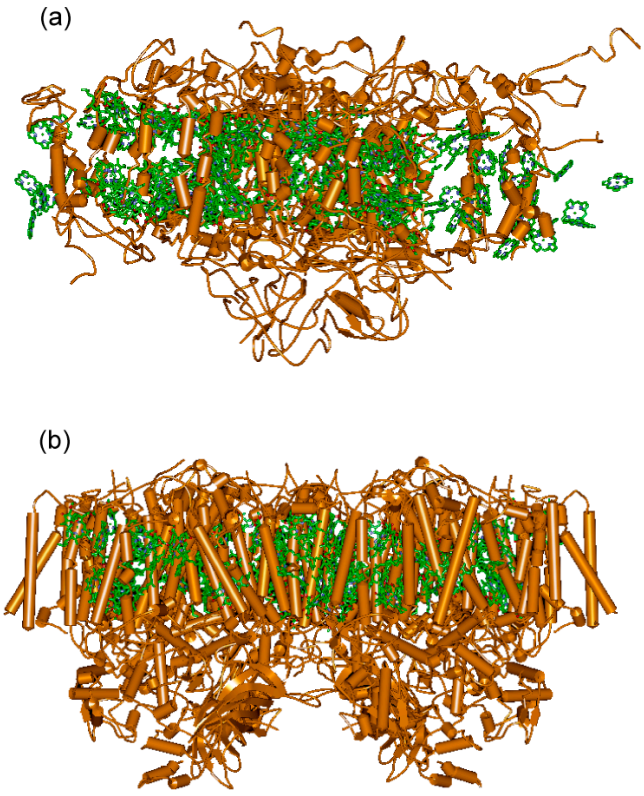

Figure 2. Crystallographic structures of (a) photosystem I and (b) photosystem II. Green molecules are chlorophylls while brown structures are the proteins. Carotenoids are omitted for clarity.

them. The remaining 90 Chl *a* are responsible for harvesting light. In addition, there are 22 carotenoid molecules in a PS I monomer (not shown). All the pigments are bound to 12 different protein units. Importantly, the Chl *a* molecules are strongly coupled, which results in a shift of the absorption wavelength of PS I (its maximum is at 700 nm), as compared to the isolated Chl *a* molecules (670 nm). On the other hand, the PS II complex is a dimer [8]. It consists of 20 protein subunits which bind 77 pigments, both Chl *a* and carotenoids. Similarly to the case of PS I, two Chl *a* molecules of PS II also form a special pair of the reaction center, although the inter-Chl coupling is somewhat weaker, with the maximum absorption of the PS II at 680 nm.

3.2. Light-harvesting complexes

Photosystem protein complexes possess a very limited capability of harnessing sunlight, both because they occupy a very small area in the thylakoid membrane and their absorption spectra are very selective. Therefore, in order to increase the amount of absorbed light, several light-harvesting antennas were developed that surround the photosystems. Their function is to harvest sunlight energy and transfer it efficiently to the reaction centers. These light-harvesting complexes are usually very specific for particular species and, as a result, a light-harvesting apparatus of a given organism is rarely able to absorb light in a very broad spectral range. For instance, the most important light-harvesting pigment, chlorophyll *a*

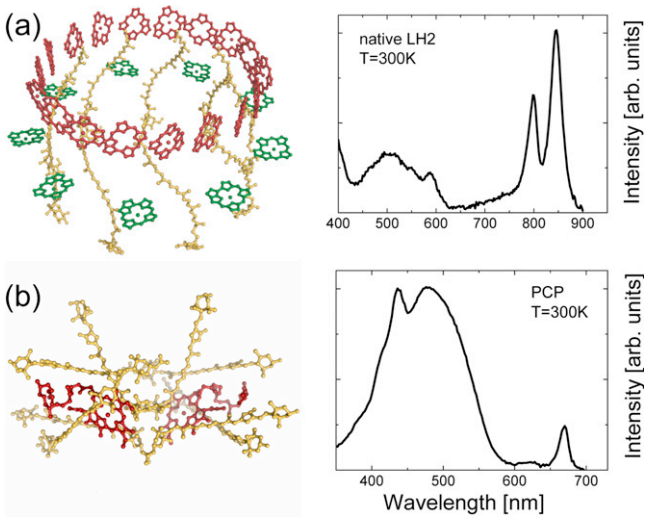

Figure 3. Pigment structures (left column) and room temperature absorption spectra (right column) of two light-harvesting complexes: (a) LH2 from purple bacteria and (b) peridinin–chlorophyll a–protein complex from dinoflagellate. B800 and B850 rings of LH2 are colored in green and red, respectively, Chl *a* in PCP is shown in red, carotenoids in yellow. Protein is omitted for clarity.

(Chl *a*), absorbs only in two spectral bands, from 350 to 440 nm and from 600 to 670 nm. As a result, there exists a huge spectral gap to which Chl *a* itself is completely blind. The light-harvesting complexes are mostly also protein–pigment complexes. The protein provides a scaffold of binding sites for the pigments, while the pigments, both chlorophylls and carotenoids, absorb the energy. Two examples of such antennas are shown in figure 3. The complex displaying a ring-like structure (figure 3(a)) is a light-harvesting complex 2 (LH2) from the purple bacteria [9]. It consists of 27 bacteriochlorophyll *a* (BChl *a*) molecules arranged in two symmetric rings and 9 carotenoid molecules embedded in a hydrophobic protein (not shown). Both the structure and the optical properties of LH2 have been a subject of intense study in recent years [10–13]. It has been shown that LH2 complexes are arranged around an LH1 light-harvesting complex, in the center of which there is a reaction center [10, 11]. The BChl *a* molecules in LH1 have a strong near-infrared absorption band of 875 nm, while LH2 has two strong BChl *a* absorption bands at 800 nm and 850 nm (figure 3(a)). In this way the energy cascade is formed, which facilitates efficient energy transfer from LH2 to LH1 complexes and then further to the reaction center. The x-ray crystallography studies of the LH2 complex have shown that, out of the 27 BChl molecules, 18 form a strongly coupled ring with average distances between the molecules less than 1 nm. This excitonically coupled ring is responsible for the absorption band at 850 nm. The remaining 9 molecules form a ring of weakly coupled BChls as they are spaced by more than 2 nm. Single-molecule investigations [13] proved that the B850 ring is, in fact, not fully symmetric and the exciton levels feature significant splitting.

The LH2 complex from purple bacteria is a very nice example to discuss qualitatively the basic characteristics of the light-harvesting antennae. The ratio of BChl to carotenoid molecules is in this case 3:1, which implies that the major light-harvesting pigment is BChl. Indeed, the absorption of the carotenoids is very weak and is located around 500 nm. Moreover, in order to ensure efficient energy transfer between the pigments, they are very strongly coupled.

In this respect, the second light-harvesting complex, peridinin–chlorophyll a–protein (PCP), is somewhat of an exception. The PCP complex is a water-soluble antenna in dinoflagellates. It is extrinsic, which means it is not located in the membrane but peripherically attached to it. The structure of the native form of PCP from *Amphidinium carterae* determined with a resolution of 2 Å revealed a trimeric system [14], a monomer of which is shown in figure 3(b). It contains two chlorophyll *a* molecules and 8 peridinin (Per) molecules which are carotenoids. All the pigments are arranged in two almost similar clusters and embedded in the hydrophilic protein capsule (not shown). The conjugated portion of each Per is close to the chlorophyll tetrapyrrole ring at a van der Waals distance (3.3–3.8 Å), the distance between Mg atoms of the two Chl *a* in one monomer is 17.4 Å and intercluster edge-to-edge distances between Per are in the range of 4–11 Å. The ratio of Per to Chl *a* of 4:1 indicates that PCP utilizes the carotenoids as its main light-harvesting pigments. It can be seen in figure 3(b), where the absorption spectrum of the PCP complex is shown. It features broad and intense bands between 400 nm and 550 nm which are predominantly due to Per absorption. The Chls *a* contribute through the band at 670 nm and the Soret band at 440 nm.

Upon absorption of light, peridinins in PCP transfer their electronic excitation to Chl *a*. The efficiency of this excitation energy transfer is higher than 90% [14]. Subsequently, Chl *a* passes the energy onto membrane-bound light-harvesting complexes and photosystem II. Clearly, the absorption spectrum of PCP enables the photosynthetic apparatus to harness the sunlight not only in the red and infrared ranges, but it extends it into the blue-green spectral region.

Optical spectroscopy studies of the PCP complex have been carried out on the ensemble and single-molecule levels. Using transient absorption in the femtosecond timescale the main energy transfer pathways have been described [15], it has also been demonstrated that the two Chl *a* molecules interact relatively weakly with a characteristic transfer time between them of the order of 12 ps [16]. These observations were also corroborated with fluorescence studies of individual PCP complexes [17]: it has been shown that it is possible to distinguish emission originating from each of the two Chl *a* molecules and, using the property of sequential photobleaching of the Chl, the energy splitting between the two molecules in the monomer were determined.

An important step towards engineering the properties of PCP complexes concerns the ability to reconstitute the protein with various chlorophylls, including Chl *b*, acetyl-Chl *a*, Chl *d* and BChl *a* [18–20]. Importantly, the folding of the protein used in the reconstitution procedure takes place over an almost identical pathway as in the native system, which results in very similar structures of the reconstituted systems [21]. Since each of these chlorophyll molecules features specific

absorption and emission characteristics, it became possible to construct and study the energy transfer dynamics as well as inter-pigment interactions in a well-defined geometry given by the protein. Indeed, the maximum absorption of these Chl molecules changes from 640 nm for Chl *b* to 760 nm for BChl *a*. Ultrafast spectroscopy revealed that the energy transfer from Per to different Chl molecules can be changed from 9.4 ps for Chl *b* to 0.5 ps for BChl *a* [19]. The dependence of the energy transfer times between Per and various Chl molecules has been applied to coherently describe the single-molecule fluorescence of PCP complexes reconstituted with a mixture of Chl *a* and Chl *b* [20].

Photosynthetic complexes developed by living organisms render themselves as an excellent system for understanding basic physical and chemical processes behind the conversion of sunlight energy. This knowledge has been used for constructing nanoscale devices able to perform either efficient energy transfer or charge separation or even both. Quite possibly, photosynthetic complexes could also be used as key elements for hybrid devices designed for converting light into usable forms of energy, such as electricity or chemical energy. Although protein structures are pretty robust, either biochemical reconstitution or genetic modifications should prove themselves sufficient to retain enough flexibility in order to tailor the hybrid system with optimized properties. When considering designing a hybrid nanostructure for the purpose of energy harnessing and conversion, it is important to take into account that the organisms which perform photosynthesis are very specific in matching their absorption needs. Their photosynthetic apparatus is not optimized for the whole range of sunlight reaching the Earth's surface. On the contrary, sets of pigments as well as the arrangement of pigment–protein complexes in the membrane is designed to be as efficient as possible in harnessing light which is available for a given organism. This strong selectivity is one of the most crucial reasons why nanoscience and nanotechnology with the ability to control the properties of matter at the nanoscale, and thus matching the scale of the pigment–protein complexes, could improve the performance of natural systems.

4. Nanostructures

Nanostructures comprise an enormous group of materials that have been the subject of very intense study over the last two decades. With tools like the scanning tunneling microscope, atomic force microscope or transmission electron microscope it has become possible to measure, understand and manipulate matter on the level of molecules and even atoms. On the other hand, with the help of technology, such as molecular beam epitaxy, electron beam lithography or reactive ion etching, fabrication of well-defined structures often with atomic precision has become an everyday experience. A natural extension of this progress has been to find ways to combine nanostructures of various origin and character in order to explore the interactions between them and design structures with better overall properties as individual components. Among most studied nanostructures which could be of importance in the context of light harvesting are semiconductor nanocrystals, and metallic nanoparticles.

4.1. Semiconductor nanocrystals

Semiconductor nanocrystals, also known as quantum dots (QDs), are nanoparticles with sizes comparable to the exciton Bohr radius in semiconductors. It translates into the range from 2.8 nm for CdSe up to 10 nm for CdTe. There have been several techniques developed for the fabrication of semiconductor QDs: these structures can be grown on a semiconductor substrate by molecular-beam epitaxy (MBE) and metal–organic chemical-vapor-deposition (MOCVD) approaches [22, 23] using strain-driven self-assembly. They are usually characterized by relatively large size and shape distributions and, due to the Stranski–Krastanov growth mode, these structures are also highly strained. Importantly, in order to reduce any negative influence of the surface (non-radiative recombination, chemical instability, etc), semiconductor quantum dots grown by epitaxy techniques must be embedded in the matrix material. Since typical capping layers used in protecting the surface of Stranski–Krastanov quantum dots is in the range of 50 nm, this poses a serious limitation for conjugating these nanostructures with other non-epitaxially synthesized systems, let alone light-harvesting complexes. Another approach is based on colloidal chemical synthesis of crystalline semiconductor nanocrystals [24–27]. These structures consist of an inorganic core coated with a layer of organic ligand molecules, which provides electronic and chemical passivation of surface dangling bonds. In this way any uncontrolled growth and agglomeration of the nanoparticles is inhibited, but more importantly, chemically synthesized nanocrystals can be manipulated like large molecules with solubility and reactivity determined by the identity of the surface ligand. This property opens many possibilities of functionalizing the nanocrystals with chemical groups, DNA or proteins required for conjugation with other nanostructures. On the other hand, very large surface-to-volume ratios result in high sensitivity of the optical properties of the nanocrystals to the surroundings. This could lead to low fluorescence quantum yield caused by non-radiative recombination of excitons at defects located at the surface. Indeed, typical fluorescence quantum yields of bare nanocrystals with ligands attached, was of the order of 10%. A breakthrough solution has been suggested in the form of overgrowing the core of the nanocrystal with a shell, typically of a semiconductor with larger bandgap energy [28]. This method has significantly improved the fluorescence properties of such prepared core/shell nanocrystals with quantum yields reaching 70%.

During the last decade colloidal synthesis of semiconductor nanocrystals has been mastered to the level where many structures can be fabricated 'on-demand' [29]. The nanocrystals feature a high degree of crystallinity, adequate surface passivation, solubility in nonpolar or polar solvents, and good size homogeneity. Moreover, it has become possible to tune the shape and chemical composition of the obtained nanocrystals. In addition to spherical particles also nanowires, nanorods, nanoprisms, nanostars, etc, were fabricated. Self-assembly of semiconductor nanoparticles into two-dimensional superstructures has also been demonstrated [30]. Such great flexibility, which would be very difficult to achieve

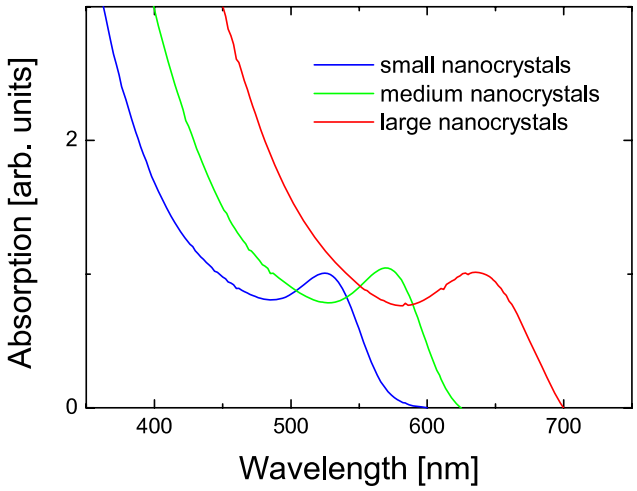

Figure 4. Schematic dependence of the absorption spectra on the size of semiconductor nanoparticles. Larger nanocrystals absorb in longer wavelengths.

with epitaxially grown quantum dots, gives the chemically synthesized nanocrystals an upper hand in terms of designing hybrid nanostructures with biological components.

Besides the considerable structural flexibility which, in principle, should sufficiently well match any specific need imposed by the particular design of a hybrid nanostructure, semiconductor nanocrystals feature a strong dependence of the optical transition energies on the crystal size. This effect, known as the quantum confinement effect, manifests itself as a continuous shift of the absorption (and fluorescence) maximum with the size of the nanocrystal [31]. This is shown schematically in figure 4. The change of the bandgap energy of the nanocrystal scales with the inverse of the squared radii of the nanocrystal. For instance, nanocrystals made of CdSe have been shown to exhibit precisely tunable emission across the whole visible spectrum by varying the crystal size. In comparison to organic fluorophores [32], inorganic semiconductor nanocrystals are characterized by greater chemical and photochemical stability and large absorption cross sections (up to 10^6 M^{-1} cm^{-1}) spanning over energies larger than their bandgap energy. In addition, their narrow emission spectrum (linewidth amounts roughly to 30 nm in the visible) in combination with superior luminescence quantum efficiencies render these nanostructures highly attractive for many optoelectronic and bioimaging applications [33, 34].

In the context of hybrid nanostructures comprising both biological and inorganic nanoscale systems, semiconductor nanocrystals present themselves as a very attractive material. First of all, the ability to functionalize the surface with various active groups, which can be used for linking the nanocrystals in a controlled way to other nanostructures, is of enormous value, as it enables precise control over the interactions between the constituents. Second, large extinction coefficients characterizing the nanocrystals should be of help in increasing the overall absorption of the system comprising a nanocrystal and a light-harvesting complex. Last, but not least, excellent tunability of the bandgap energy with either the choice of material or the size and shape of the nanocrystal, gives a unique possibility to fill the spectral gaps of the natural light-harvesting complexes.

4.2. Metal nanoparticles

Metallic nanoparticles are complementary nanostructures to the previously discussed semiconductor nanocrystals. While the semiconductor nanocrystals, at least in their standard form, contain no free carriers, metal nanostructures are characterized with a high concentration of electrons. Thus, illumination with the laser leads to the formation of plasmon excitation: a wave of free electrons [35]. In contrast to plasmons excited in bulk materials, in the case of metallic nanoparticles of sizes less than or comparable to the wavelength of light, the plasmon excitation possesses local character. Therefore, such a nanostructure resembles an additional source of local electromagnetic field. This unique property of metal nanoparticles is the main reason why these systems have generated great interest in recent years in many, often very diverse, research fields such as optical spectroscopy, cell imaging, quantum information processing, nanophotonics and biosensors [36–42]. Such a broad range of applications results from the influence that plasmon resonances excited in metal nanoparticles impose on dipoles localized in their vicinity. An isolated dipole (emitter) is characterized by three parameters: excitation rate, which is the efficiency of promoting the molecule to the excited state, radiative rate, which is the probability of emitting a photon while relaxing back to the ground state, and non-radiative rate, which describes radiationless losses, as displayed in figure 5(a). When placing such a dipole close to the metallic nanoparticle, all these rates are affected by the presence of the plasmon [32]. The influence of the plasmon is represented by the additional channels both for the excitation as well as the emission in figure 5(b). Additionally, since metal nanoparticles are very efficient in dissipating energy, another process has to be taken into account when analyzing the plasmonic interaction with the emitter: non-radiative energy transfer from the emitter to the metal nanoparticle. This process is radiationless; it is converted mainly to heat in the metal. In other words, enhanced electromagnetic fields near metallic nanostructures can alter, due to localized plasmon resonances, the optical properties such as fluorescence intensity and lifetime of fluorophores placed in their vicinity. The energy transfer to metal nanoparticle results in a very efficient quenching of the fluorescence. In contrast, increase of both the excitation rate and radiative rate is behind an effect called metal-enhanced fluorescence (MEF) [42], as it leads to an increase of the fluorescence emission accompanied with a decrease of the fluorescence lifetime. The actual net effect of the plasmon excitation on the optical properties of an emitter depend crucially upon the geometry of the system and the optical properties of the constituents [41]. Particularly important are the size and shape of the metal nanoparticle, distance and relative orientation of the emitter–plasmon system as well as spectral characteristics of the plasmon, i.e. energy and linewidth of plasmon resonance and absorption and emission spectra of the emitter.

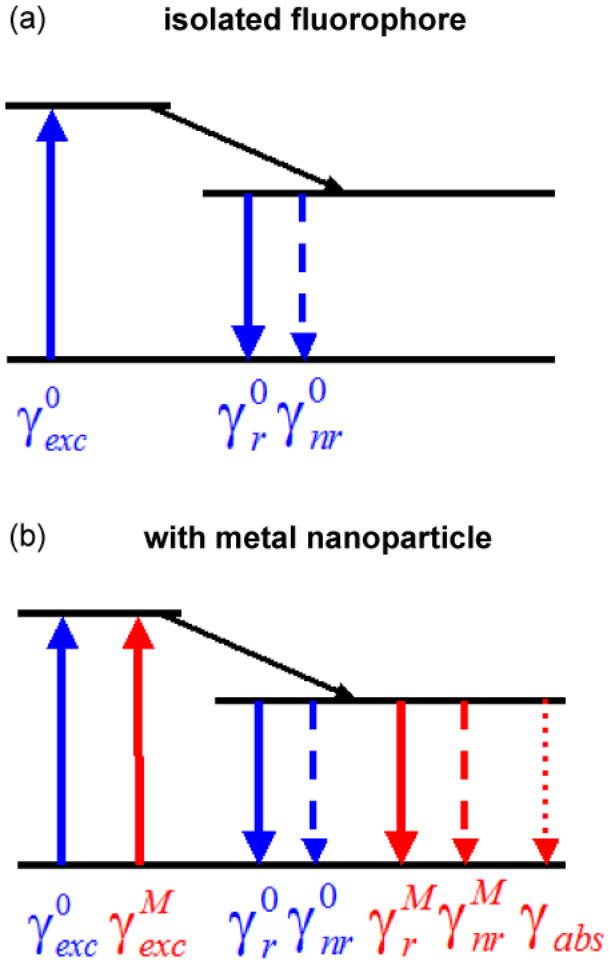

Figure 5. Schematic representation of the influence of plasmon excitation in a metallic nanoparticle on the optical properties of a fluorophore. (a) An isolated fluorophore is characterized with the excitation rate ($\gamma^0_{\rm exc}$), radiative rate (γ^0_r) and non-radiative rate (γ^0_{nr}). (b) Due to plasmon interaction not only are all three rates modified ($\gamma^M_{\rm exc}$, γ^M_r and γ^M_{nr}), but there is an additional process due to energy transfer from the fluorophore described with the rate $\gamma_{\rm abs}$.

Remarkable progress has been made in the design of metal nanostructures, which is essential for tuning the resonance frequency and thus the coupling strength. Complementary efforts focused on developing advanced experiments to study dipoles placed in the vicinity of a metal nanoparticle have shed light on the interplay between radiative and non-radiative processes in these systems. The first method of obtaining metal nanostructures with defined geometry has been electron beam lithography [43, 44], including evaporation and lift-off. This approach allows for precise positioning and shaping of nanoparticles on the substrate: however, controlling the quality as well as the chemistry of the metal surface frequently proves challenging. An important limitation is also related to the technological expertise required for reproducible fabrication of metallic nanoparticles. A much more common approach, similarly as in the case of semiconductor nanocrystals, is synthesis based on colloidal chemistry that has been seeing great progress in preparing nanoparticles with various sizes, shapes and even chemical composition [45–47]. It has been

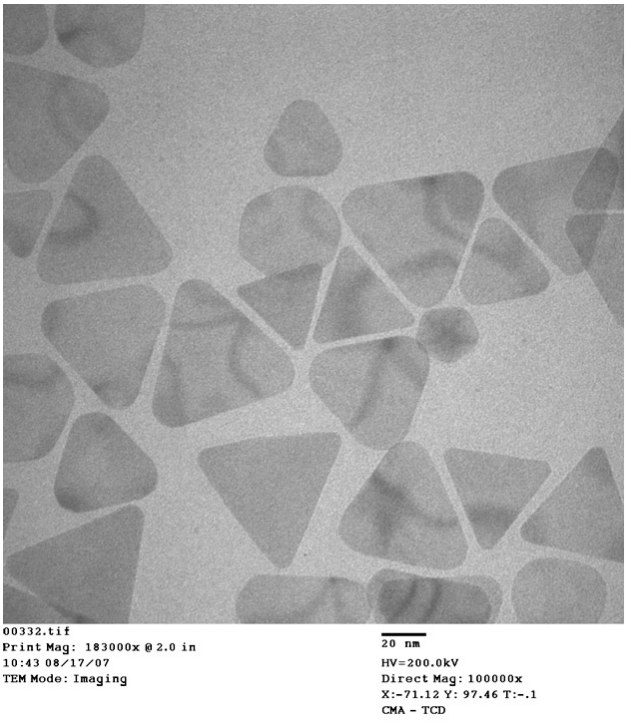

Figure 6. Transmission electron microscopy image of silver nanotriangles.

particularly important in the case of silver, whose quite high reactivity would easily worsen the structural quality and thus possible implementation in plasmon-based devices. In order to protect the surface, a very thin gold shell has been synthesized to surround the silver nanoparticle [48]. An example of chemically synthesized metallic nanotriangles is shown in figure 6 [49].

The most important characteristics of metallic nanoparticles are the energy and the linewidth of the plasmon resonance as they define the spectral range of plasmon interaction with a nearby dipole. Again, analogously to semiconductor nanocrystals, both the size and the shape of nanoparticles define the plasmonic properties of nanostructures. It has been shown that by increasing the diameter of gold spheres from 20 nm to 150 nm it is possible to shift the resonance from the blue to red side of the visible spectrum [50]. The dependence measured for silver spheres seems a little narrower. However, metallic nanoparticles with larger sizes feature resonances with very broad linewidths. For instance, plasmon resonance obtained for silver spheres with a diameter of 80 nm could be as broad as 800 meV [50]. Such strong broadening, which is a result of much shorter dephasing times in metallic nanoparticles with larger sizes, was thought to diminish the possibility of using these structures for precise tuning plasmon resonances to the desired wavelength region. This limitation has been overcome by fabrication of gold nanoparticles in the form of nanoshells [51], whose plasmon resonances can be shifted into the near-infrared. A similar effect has been observed for nanotriangles made of silver, as displayed in figure 7, where scattering spectra of silver nanotriangles with increasing edge length are shown. Furthermore, plasmon

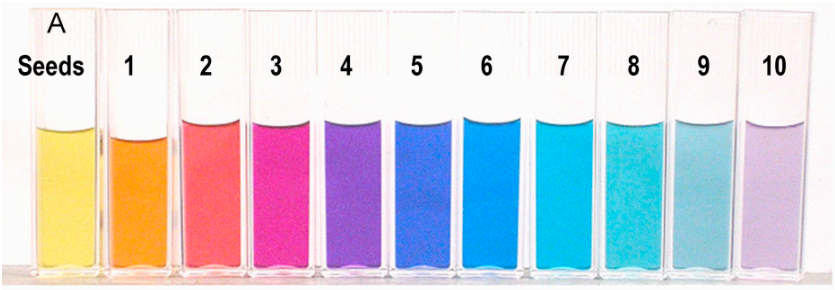

Figure 7. Photograph of a series of samples containing silver nanotriangles that illustrate the tunability of plasmon resonances in these structures.

engineering can be extended by designing nanostructures with two plasmon resonances at different energies, which is the case of nanorods [45]: one plasmon frequency located at higher energy is associated with resonance perpendicular to the nanorod axis, while the second one is due to resonance along the axis. It appears at lower energies, often in the near-infrared region of the electromagnetic spectrum.

The complex nature of plasmon interactions with emitters and/or absorbers is due to how the presence of metallic nanoparticles affects the excitation and radiative rates of the molecule with addition of the energy transfer process which results in fluorescence quenching. In a classic experiment [41] which shows the full range of possible configurations, a single gold nanosphere was attached to the end of an optical fiber and placed above a single molecule of Nile blue dye. The experimental set-up allowed for precise control of the distance between the dye and the nanosphere from just a few nanometers up to 100 nm. As the distance was changed, the fluorescence intensity of the dye emission was recorded. Three different regions were identified in the fluorescence intensity dependence upon the distance between the molecule and the metal nanoparticle. For the distances larger than 40 nm the intensity was identical to the one of the isolated dye molecule. As the distance was reduced, the fluorescence intensity started to rise, as a result of the increase of the fluorescence quantum yield and excitation rate. Further decrease of the separation between the two nanostructures resulted in fluorescence quenching due to energy transfer from the dye molecule to the metal nanoparticle. A maximum of the fluorescence enhancement ($\sim$ fivefold increase) was observed at a distance of about 8 nm.

Although the exact mechanism of MEF is not fully understood, it has been demonstrated that properly designed geometry can result in significant enhancement of the fluorescence. Most of the time, the observed increase of the emission is a combination of the enhancement of the fluorescence quantum yield and the excitation rate. One of the challenges regarding implementing plasmon interactions in hybrid devices comprising natural light-harvesting complexes should be finding a way to separate these two contributions and proposing a device where the enhancement of the excitation rate would play the dominant role.

5. Energy transfer between nanocrystals

Energy transfer between pigments in photosynthetic complexes is, besides the light harvesting and charge separation, one of the most important physical processes that determine the function of the photosynthetic apparatus. It defines how efficiently the excitation is funneled down to the reaction center and what is the sensitivity and the spectral range of the photosynthetic apparatus. The simplest artificial (inorganic) system which has been used to study the energy transfer consisted of two molecules, one of which plays the role of the energy acceptor while the other is a donor. There are in principle three requirements for such a system for energy transfer to take place: the emission of the donor should partially overlap with the absorption of the acceptor, the distance between the two molecules should be of the order of 10 nm, and the dipole moments of these molecules should not be perpendicular to each other. Under such conditions, the energy transfer is described by the well-known Förster equation [32]:

$$k_T(r) = \frac{9000(\ln 10)\kappa^2\Phi_D}{128\pi^5 N_A n^4 \tau_D R^6}\int_0^\infty F_D(\lambda)\varepsilon(\lambda)\lambda^4\,d\lambda,$$

where κ is an orientation factor, Φ_D and τ_D are the fluorescence quantum yield and the fluorescence lifetime of the donor, n is the refractive index of the solvent and R is the distance between the donor and acceptor. The integral describes the overlap between the absorption spectrum of the donor and the fluorescence spectrum of the acceptor.

Based on this principle, molecular complexes have been designed to absorb light and transfer the energy to the energetically lowest-lying molecule [52, 53]. The chemical synthesis has opened the possibility to construct artificial light-harvesting systems, which mimicked the functionalities of their natural counterparts, including energy and electron transfers. These supramolecular complexes, instead of just two molecules, contained many various molecules with well-designed spectroscopic properties. Most often chlorophyll derivatives, porphyrins and carotenoids have been used. In addition to careful selection of the molecules, the geometrical architecture also played an important role in these artificial systems: they feature dedrimeric structures with the energetically lowest-lying molecule in the center of

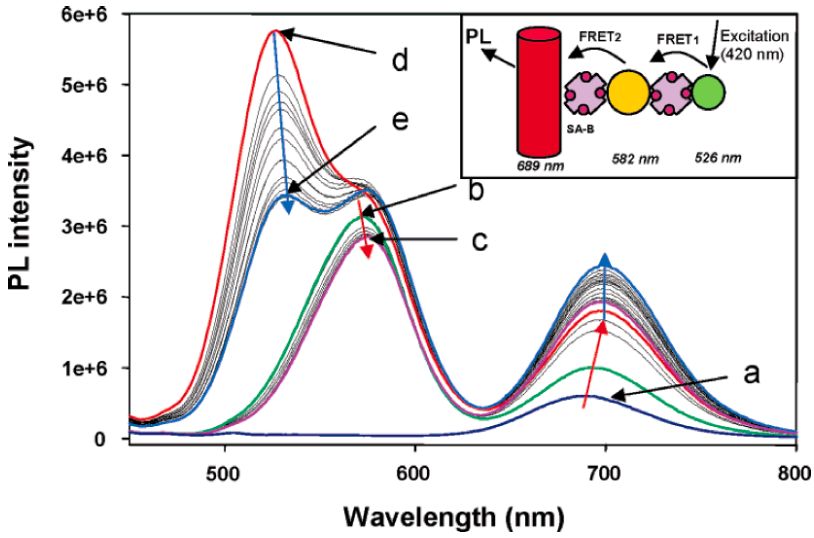

Figure 8. Fluorescence spectra of multiconjugated semiconductor nanoparticle superstructures: a—only nanowires; b—nanowires conjugated with orange nanoparticles; c—after 21 min of the reaction; d—upon adding green nanoparticles; e—after 30 min of the reaction. Arrows indicate the progression of spectra with time as bioconjugation reactions proceed. Red arrows correspond to the initial formation of nanowire–orange nanoparticle conjugates. Blue arrows correspond to spectral changes started after addition of green nanoparticles to the formed assembly. In the inset a schematic of the multiple conjugated nanowire–nanoparticle superstructure is shown. (Reprinted with permission from [56]. Copyright 2005 American Chemical Society.)

it [53]. This central molecule was then surrounded by several other molecules, whose function was to harvest light and subsequently transfer it down. A certain limitation of this approach concerns the relatively narrow absorption bands of organic molecules. Therefore, to facilitate the energy transfer between different molecules, great care had to be taken to ensure the spectral overlap between the emission of the donor and the absorption of the acceptor. Furthermore, artificial light-harvesting systems based on molecular constructs contain many different molecules in order to absorb light from a broad wavelength range.

Some of these issues could be overcome by using semiconductor nanocrystals as light-harvesting nanostructures, in particular when considering very high extinction coefficients and spectral tunability due to quantum size effects. The challenging aspect of this approach concerns controlled assembly of nanocrystals with various sizes (and thus absorption energies) in a structure where the distance between acceptors and donors is in the range of 10 nm. The first successful attempts applied layer-by-layer deposition of nanocrystals with different sizes [54, 55]. Very efficient transport of excitons from green-emitting nanocrystals to red-emitting NPs have been deduced in such structures from substantial quenching of green luminescence in gradient films [54]. Another step towards applying semiconductor nanostructures for light harvesting has been made by fabricating a superstructure from spherical nanoparticles and elongated nanowires [56]. Two sets of CdTe nanocrystals with diameters of approximately 3 nm (green nanoparticles emitting at 526 nm) and 4 nm (orange nanoparticles emitting at 582 nm) were used; they constitute a very efficient energy transfer pair. As the energetically lowest-lying nanostructure a CdTe semiconductor nanowire was used with a diameter of 6.6 nm and typical length of 500 nm. The maximum of the fluorescence emission of the nanowires was at 689 nm. The purpose of such designed systems was to observe the cascade energy transfer from the green to orange nanocrystals and further to the nanowires.

Instead of using layer-by-layer self-assembly to construct a structure where the components would reside at distances which promote the energy transfer, bioconjugation has been used. The assembly was a two-step process: first, nanowires dressed with biotin were mixed with the orange nanocrystals dressed with streptavidin. The pair of biotin and streptavidin is a very common protein combination used for biolinking various materials: they have a very high affinity to bind with each other. The reaction of the formation of nanowire–orange nanoparticle complexes was monitored using fluorescence spectroscopy: as bioconjugation progressed, the intensity of the nanowire emission increased due to the energy transfer from the nanoparticles. Once saturated, it was an indication that all the nanoparticles were attached to the nanowire. In the next step the green nanoparticles dressed with biotin were added to the solution [56] in order to bioconjugate with the orange nanocrystals already attached to the nanowire. The result of this experiment is shown in figure 8, where fluorescence spectra are displayed as both reactions progressed. The energy transfer from the orange nanocrystals to the nanowires leads to the increase of the nanowire fluorescence. Upon including the green nanocrystals, the fluorescence of the nanowires increased further, which is an indication of the cascade energy transfer.

The superstructure designed by bioconjugating properly selected semiconductor nanoparticles provides a model system for understanding the energy transfer and its dependence upon excitation wavelength as well as polarization of light. It is important to note that the nanoparticles used in this experiment allow for efficient absorption of light in a very

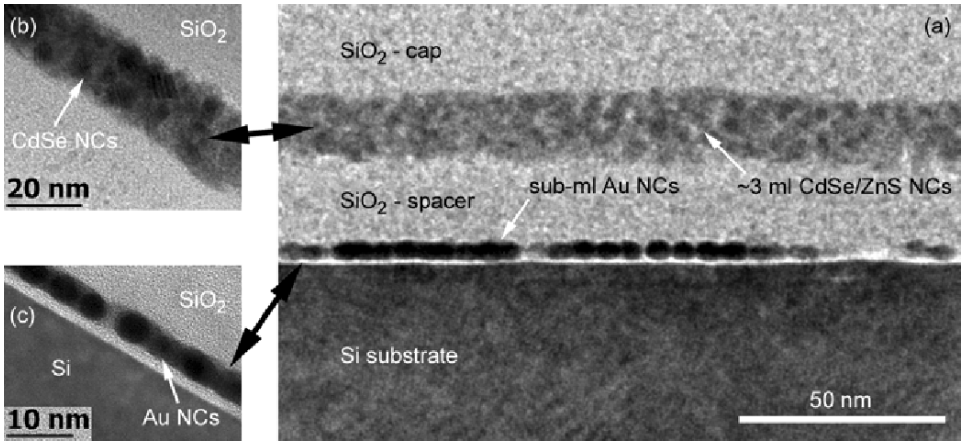

Figure 9. (a) Transmission electron micrograph of a sample with a 15 nm thin SiO_2 spacer layer separating gold nanoparticles and semiconductor nanocrystals. (b) and (c) show a high-resolution image of the CdSe/ZnS and the gold nanocrystal film.

broad spectral range. Also, applying semiconductor nanowires, which could be conductive, opens a possibility to convert the harvested exciton into current. It is important to note that the nanoparticles used in this experiment allow for efficient absorption of light in a very broad spectral range.

6. Metal-enhanced fluorescence

6.1. Semiconductor nanoparticles

As discussed previously, plasmon resonances excited in metallic nanoparticles affect the optical properties of dipoles located in their vicinity. Although most studies regarding the interaction between plasmons and emitters have been carried out on organic fluorescent dyes [38, 41, 57, 58], there are also reports on the fluorescence of semiconductor nanocrystals coupled to metal nanoparticles [42, 59–61]. One of the studies focused on CdTe nanocrystals coupled to a film of silver islands, SIF [42]. The islands formed as a result of the reduction of an aqueous silver nitrate solution, they were very inhomogeneous in sizes and shapes and the nanocrystals were spread over the SIF surface in a thin polymer film. Ensemble fluorescence spectroscopy of such a prepared sample featured a sixfold increase of the fluorescence intensity accompanied by a shortening of the fluorescence lifetime. These observations were interpreted as a result of an increase of radiative rate in the nanocrystals [42]. Single-molecule spectroscopy measurements carried out on a similar system, but diluted strongly enough to make the experiments on single nanocrystals possible, confirmed the ensemble data. At the same time, however, it has been found that the enhancements of the intensity varies considerably between individual nanocrystals, as indeed expected due to substantial inhomogeneities in the structure due to size and shape distributions of silver islands as well as the variation of the relative distance between the nanocrystals and the SIF. Clearly, in order to quantify the observed effects it was necessary, as in the case of semiconductor nanoparticle assemblies, to control the separation between metal nanoparticle and emitter. Straightforwardly enough, bioconjugation with the biotin–streptavidin linker has been used to couple gold nanoparticles with CdTe nanowires [61]. In such a configuration the ensemble fluorescence of the nanowires increased by a factor of 6. However, no experiments on single nanowires were performed, therefore, it is not clear how homogeneous was the synthesized hybrid structure.

Nowadays, nanotechnology and processing of materials provide excellent ways to control matter at the nanoscale. An example of a hybrid nanostructure fabricated using the electron beam evaporation technique is shown in figure 9 [62]. It displays an Si wafer on which a monolayer of uniform gold nanoparticles with diameters of 4–5 nm was spin-coated. Next, a precise layer of SiO_2 with a thickness of 15 nm was evaporated with an electron beam. On top of such a prepared sample CdSe/ZnS core/shell semiconductor nanocrystals were again spin-coated to form a uniform layer. The maximum of the fluorescence emission of the nanocrystals was at 620 nm while the maximum of the absorption was at 575 nm, which matches almost ideally the maximum of the plasmon resonance of the gold nanoparticles [62]. The precision of thickness control in this sample is remarkable (figure 9(a)). In order to determine the influence of plasmon excitations in the gold nanoparticles on the fluorescence of the nanocrystals, a series of otherwise identical samples with different SiO_2 thickness was fabricated. In figure 10 we show the integrated intensity of the ensemble fluorescence measured as a function of the spacer thickness. The error bars originate from multiple measurements at different spatial positions across the structure and the results are compared to the reference sample containing nanocrystals only (dashed line). The behavior of the fluorescence intensity is quite similar to the results described in [41]: for separating layers thicker than 25 nm the emission approaches the reference level, while for shorter distances a clear increase of the fluorescence intensity can be observed. The largest increase of the intensity has been obtained for the spacer of 10 nm. Below this value the emission decreases. The architecture of the sample shown in figure 9 is very attractive for possible application in light harvesting, mostly due to the excellent control over

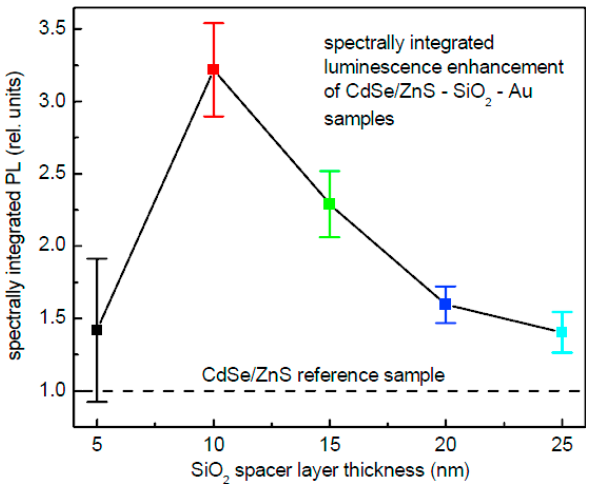

Figure 10. Magnitude of spectrally integrated photoluminescence of samples with separation distances between the CdSe/ZnS film and the gold nanocrystal layer of 5, 10, 15, 20 and 25 nm (squares). The values are normalized with respect to the integrated spectrum of the CdSe/ZnS reference sample and represent therefore the enhancement factor for spectrally integrated luminescence.

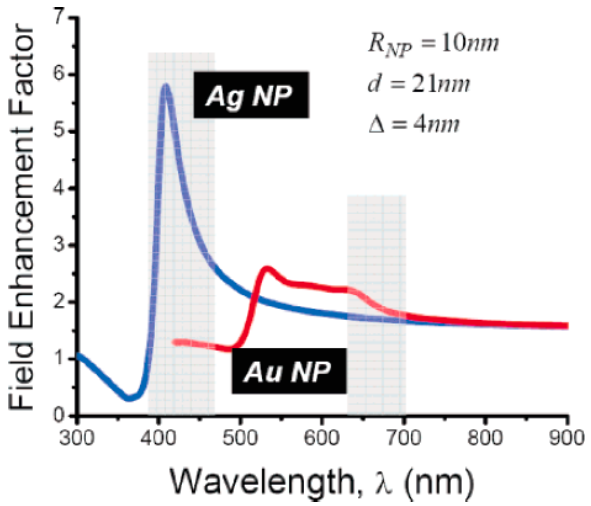

Figure 11. Calculated enhancement factors for Au and Ag metallic nanoparticles with diameters of 21 nm as a function of the wavelength. Shaded areas correspond to the main absorption bands of Photosystem I. (Reprinted with permission from [64]. Copyright 2007 American Chemical Society.)

the morphology of the structure and possibility to design and prepare a multilayer, multifunctional assembly.

6.2. Photosystem I

Following the considerable progress in understanding plasmon interactions with dye molecules and semiconductor nanocrystals, which are single dipoles, efforts have been made to study more complicated systems containing larger numbers of dipole moments. This could also include structures featuring energy transfer between the dipoles. As for the initial attempt, the relatively simple approach has been adopted, namely, using the silver island film applied previously to semiconductor nanocrystals [42]. Preliminary experiments have been carried out on photosystem I deposited close to the SIF. Since this photosynthetic complex exhibits almost no fluorescence at room temperature, the experiments were performed at cryogenic temperatures of 1.4 K with an excitation wavelength of 680 nm. The results indicated that the emission of PS I, which appears at approximately 700 nm, has indeed been enhanced around 30 times. However, since a PS I monomer contains almost a hundred Chl *a* molecules, some of which are strongly coupled while the others are interacting only very weakly, implying various complicated energy transfer pathways, the interpretation of these experiments has been quite difficult [63].

Interactions between photosystem I and metallic nanostructures have been a subject of recent theoretical studies where electromagnetic field enhancements as well as electron production rates were estimated [64]. It has been found that, due to plasmon interaction, it is possible to significantly enhance the efficiency of chemical energy production of a photosynthetic system. As discussed above, the net effect is the result of competition between enhancement of the electromagnetic field and the energy transfer from photosystem I to the metallic nanoparticle. In figure 11 we show the electromagnetic field enhancement calculated for gold and silver nanoparticles with a diameter of 20 nm as a function of wavelength. In the case of gold nanoparticles, the maximum enhancement appears in the wavelength range from 550 to 650 nm, while for the silver nanoparticle there is a much stronger resonance at about 420 nm. It is, of course, important to compare the maxima of the electromagnetic field enhancement with the absorption spectrum of the PS I complex, which is represented by the gray areas in figure 11. While for the silver particle there is significant overlap between the wavelength range for which the maximum electromagnetic field enhancement appears, the plasmon resonances calculated for the gold nanoparticles show almost no matching with the absorption of photosystem I. This result strongly suggests that silver nanoparticles of this particular size are far more suitable for changing the optical properties of the photosynthetic complex considered here. However, none of these nanostructures exhibit significant overlap with the most intense absorption band of photosystem I, which is around 680 nm. In order to induce resonance between the plasmon frequency and absorption maximum of the light-harvesting complex it turned out to be necessary to modify the morphology of the metallic nanoparticle. In the same work, the calculations were extended into metallic nanoparticles in the form of nanoshells [64] which are known to feature plasmon resonance in the red and infrared spectral ranges, depending upon the exact geometry. Indeed, calculated dependences of the electromagnetic field enhancement in the vicinity of both gold and silver nanoshells show strong maxima around 680 nm [64]. The enhancement factors obtained for silver and gold nanoshells at wavelengths around 680 nm were equal to 15 and 10, respectively. On the other hand, in the case of silver spherical nanoparticles the maximum enhancement of 6 appears at 420 nm. The results of calculations carried out for hybrid nanostructures

composed of metal nanoparticles and photosynthetic complexes provide a very nice example of spectral tunability available with inorganic nanoparticles. As a consequence, the rates of electron production in photosystem I placed in the vicinity of properly designed metallic nanoparticles could be increased by an order of magnitude as compared to the isolated photosynthetic complex. This theoretical prediction provides compelling evidence that hybrid nanostructures could potentially outperform natural photosynthetic complexes in their native environment.

6.3. Peridinin–chlorophyll–protein

Peridinin–chlorophyll–protein is a light-harvesting complex which contains only two Chl *a* molecules and eight Per molecules; therefore, it is less complicated than PS I. Moreover, the spectral properties of PCP, as discussed above, including significant overlap between Per absorption and plasmon frequencies of metal nanoparticles, renders PCP an ideal system for studying the impact of plasmonic interactions on the excitation and recombination dynamics in this relatively simple light-harvesting biomolecule. These results will be described in greater detail.

PCP complexes were obtained by biochemical reconstitution of the N-terminal domain apoprotein with Per and Chl *a*, as described in detail previously [18]. The final product, monomeric PCP reconstituted with Chl *a*, was equilibrated with TRIS buffer (5 mM, pH 7.6) and kept frozen until used.

Silver island films (SIFs) were prepared by reducing an aqueous silver nitrate solution [5, 42]. All chemicals were purchased from Sigma-Aldrich and used as received. Freshly prepared aqueous NaOH (1.25 M) was added to a silver nitrate solution. The precipitate was re-dissolved by adding NH_4OH, and the solution was cooled to ∼5 °C under stirring. After adding D-glucose, clean microscope cover slips were dipped in the solution, which was then heated up to 30 °C. The resulting Ag-covered glass cover slips were examined using absorption spectroscopy and atomic force microscopy (AFM). The AFM image of the SIF sample shows highly inhomogeneous metal islands with diameters in the range of 70–140 nm and heights between 30 and 40 nm. The absorption spectrum of the SIF sample is compared with the absorption spectrum of the PCP complex in figure 12: it features a plasmon resonance at about 420 nm and a linewidth of about 150 nm, which matches nicely the PCP absorption [5].

The major experimental technique used to analyze the spectroscopic properties of PCP complexes coupled to SIF was single-molecule fluorescence at room temperature. The emission of Chl *a* in a PCP complex is characterized by the fluorescence quantum yield of ∼30% and lifetime of ∼3.7 ns [20]. The measurements were performed at room temperature using a modified scanning confocal microscope (Zeiss LSM 410) equipped with a high NA (1.4) oil-immersion objective. The samples were excited at 532 nm, which corresponds to the absorption of Per molecules. Therefore, we utilize the efficient energy transfer between Per and Chl to observe fluorescence of PCP [65]. The emission was extracted using band pass filters, dispersed

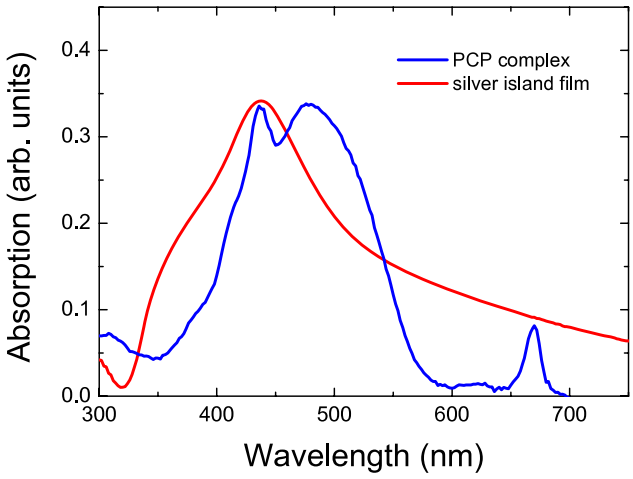

Figure 12. Comparison between absorption spectra of PCP complexes (blue) and the silver island film (red).

by an Amici prism and detected by a Peltier-cooled CCD camera (Princeton Instruments, EEV 1300/100-EMB chip) with exposure times of 0.3 s. The experimental set-up allows one to measure a 30 × 30 μm image using the APD detector as well as the fluorescence spectra using the CCD chip. Desired concentrations of the light-harvesting complexes were achieved by diluting the PCP solution in 2% aqueous PVA solution. For the experiments a 20 μl drop of the sample was spin-coated on the SIF cover slips. Samples prepared on bare glass cover slips in exactly the same way were used as reference. The thickness of the PVA layer containing PCP complexes was about 100 nm. Fluorescence lifetimes were measured with a time-correlated single-photon counting technique. In this case, a 530/10 nm bandpass filter was used to select the excitation wavelength from the white light supercontinuum given by a Ti:sapphire laser (Coherent Mira, 150 fs pulse width, 75.3 MHz repetition rate). The excitation beam was guided into the microscope (Nikon Eclipse TE2000-S) and focused onto the sample using an oil-immersion objective (Nikon Plan Fluor S, NA = 1.3). The sample fluorescence spectrally filtered with a 670/10BP filter was detected with a fast APD detector (APD-MPD-5CTC PicoQuant, FWHM of ∼27 ps).

In figure 13(a) we show the fluorescence spectra obtained for PCP complexes at ensemble concentration deposited on SIF substrates. For comparison, we also include a spectrum obtained for PCP complexes deposited directly on a standard glass cover slip. The excitation wavelength in both cases was 532 nm, which corresponds to the absorption of Per. The results obtained for the PCP ensembles suggest that the fluorescence emission of the light-harvesting complexes on the SIF is enhanced considerably, by a factor of six, as compared to the spectrum measured for the PCP on a glass substrate. We tentatively attribute this enhancement to the local increase of the electromagnetic field due to plasmons excited in metal islands. This interpretation is supported by the data shown in figure 13(b), where the photobleaching characteristics are presented for PCP complexes. The traces were obtained by acquiring the sequences of the fluorescence

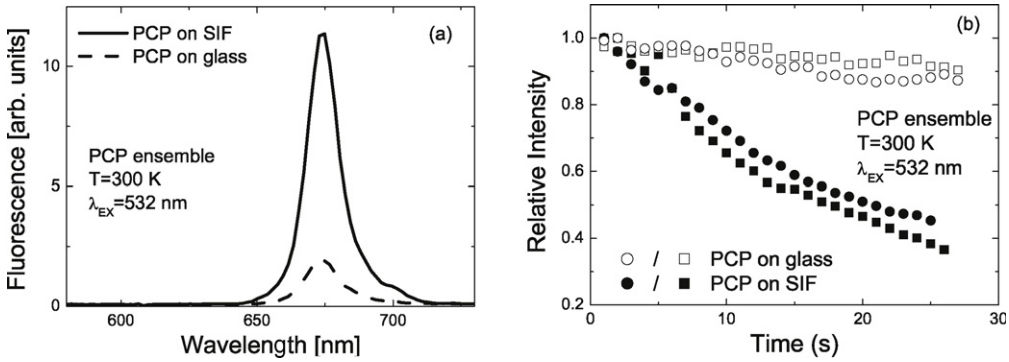

Figure 13. (a) Average fluorescence emission spectra measured for PCP ensembles on bare glass (dashed line) and SIF-coated cover slips (solid line) excited at 532 nm. (b) Temporal evolution of the fluorescence intensity of PCP ensembles on bare glass (open symbols) and SIF-coated cover slips (solid points). The excitation wavelength was 532 nm.

spectra for PCP deposited on SIF (solid points) and directly on the glass surface (open points) with two datasets measured for each configuration. The emission intensity of the reference sample decreases by ∼10% over the first 30 s; that of the PCP complexes coupled to SIF decreases during this time by ∼50%. The fluorescence intensity of the PCP complexes coupled to plasmons decreases much faster than that of the bare ones, which may suggest molecules in the vicinity of a metal nanoparticle undergo more photocycles per second. Higher numbers of absorption and emission events should lead to a more rapid decrease of the fluorescence intensity.

Although the results shown in figure 13(b) provide a clear distinction between PCP complexes coupled and uncoupled to plasmon excitations localized in SIF, there exists a serious drawback of the ensemble experiment and it is related to our inability to precisely determine the exact concentration of light-harvesting molecules excited with the laser. The fabrication of the sample involves spin-coating, which could easily result in fluctuations of the actual concentration of PCP. Therefore, in order to correctly interpret mechanisms of interactions between plasmon excitations and fluorophores it is necessary to study these effects on a single-molecule level [41, 42]. The typical fluorescence spectra of single PCP complexes placed on glass and SIF surfaces are displayed in figure 14. The average fluorescence enhancement observed for these complexes is, similarly to the ensemble data, sixfold. Importantly, analysis carried out for over a hundred single PCP molecules reveals that the distribution of fluorescence intensities measured for PCP on a glass substrate is much narrower than for these measured on SIF substrates [5]. In the first case the values range from 50 to 270 counts with 0.3 s acquisition time with an average value of 90. Remarkably, for PCP complexes deposited on SIF the fluorescence intensities vary from 60 to almost 2000, with an average value of 540 [5]. This result is similar to previously published experiments for CdTe nanocrystals on SIF [42]; it is a clear indication of inhomogeneities (or heterogeneities) within the sample. One of the possible sources of these heterogeneities is the distribution of distances between a given PCP complex and a metal nanoparticle which, in this case, ranges from essentially zero to 100 nm (which is the thickness of the PVA layer in which PCP complexes are embedded). Therefore, a broad distribution

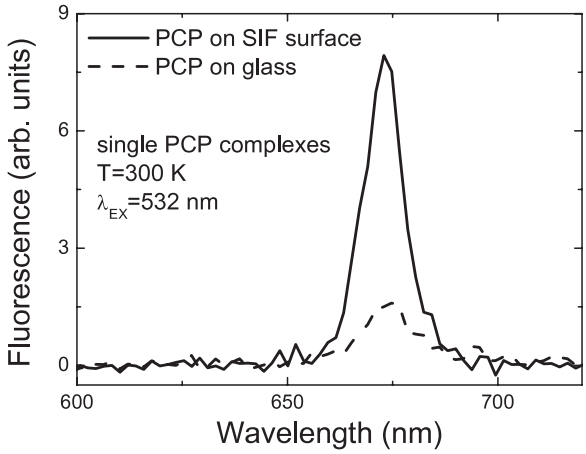

Figure 14. Typical fluorescence emission spectra measured for single PCP complexes on bare glass (dashed line) and SIF-coated cover slips (solid line). The excitation wavelength was 532 nm.

of fluorescence intensities is expected, as the fluorescence enhancement strongly depends upon the distance between metal nanoparticle and emitter. Another factor contributing to the broad distribution of observed fluorescence intensities is the variation in size of Ag nanoparticles. It is well known that the maximum of plasmon resonance and, therefore, the electromagnetic field enhancement depends upon the size of the nanoparticle [66]. Nevertheless, the results of fluorescence spectroscopy obtained for PCP complexes on an SIF substrate demonstrate that plasmons in silver nanoparticles could lead to a very large enhancement of the fluorescence intensity. This result opens a way to tune the optical properties of complex systems, such as light-harvesting antennae, by means of plasmon engineering.

Valuable information about the exact mechanism of fluorescence enhancement and relative contributions of non-radiative and radiative processes can be deduced from the excited state dynamics of the Chl emission. In figure 15 we compare the fluorescence decay of PCP complexes on SIF with that of the reference sample. The fluorescence signal of PCP on glass decays mono-exponentially with a lifetime of $\tau = 3.68$ ns, which is typical for Chl emission in PCP. Conversely,

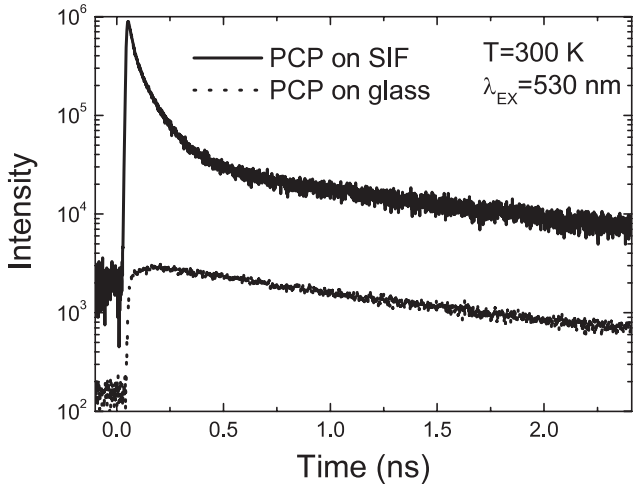

Figure 15. Time-resolved fluorescence of PCP on bare glass (dotted line) and SIF-coated cover slips (solid line). The excitation wavelength was 530 nm and the pulse width was 150 fs.

the fluorescence of PCP complexes deposited on SIF decays much faster and features multiexponential behavior: the lifetime of the high-intensity component is as short as 200 ps. At later times the trajectory gradually approaches that of PCP on glass cover slips; at times >1 ns both curves are parallel to each other. Since the non-radiative energy transfer that takes place between PCP complexes and metal nanoparticles that are within 5 nm from each other is extremely fast [57], it should be characterized with a decay time comparable to or even shorter than the internal response function of the experimental set-up. Therefore, PCP complexes that feature decay times between 200 ps and 3.68 ns should be coupled to the metal islands and, as a result, have their radiative and non-radiative lifetimes affected. The complicated, multiexponential behavior is another aspect of the aforementioned sample heterogeneity, with contributions from PCP complexes interacting with metal nanostructures of different sizes, as well as the distribution of the interaction strength due to changes in distances between the SIF layer and the pigments in the complex.

In order to figure out which of the mechanisms played the most important role in enhancing the fluorescence of the PCP complexes, it is sufficient to notice the remarkably large overlap between the absorption spectrum of the light-harvesting complex and the plasmon resonances of the SIF. This overlap is much larger than that corresponding to the fluorescence emission of the Chl molecules embedded in the complex. Based upon only this very qualitative observation, we anticipate the increase of the absorption of the PCP complex is the most dominant effect responsible for higher fluorescence intensities measured for PCP coupled to the SIF. This hypothesis has been verified by recent theoretical calculations [5].

A natural step towards controlling the plasmon enhancement in biomolecules to a larger degree would be to study analogous effects for systems with metal nanoparticles of defined geometry. Such experiments should not only extend the present understanding of the plasmon effect on the light-harvesting complexes, but can be important for

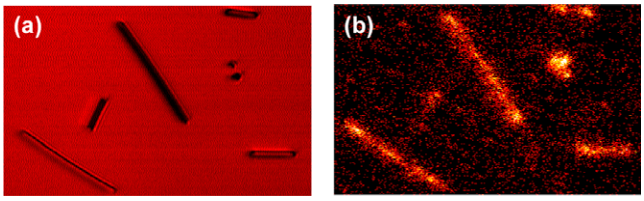

Figure 16. Representative data obtained for PCP complexes mixed with Ag nanowires. (a) Transmission image of the nanowires. (b) Fluorescence image of the same sample area. Brightness of the spots corresponds to the intensity of the fluorescence emission. The excitation wavelength was 532 nm. The horizontal size of the images is 30 μm.

developing theoretical models describing electromagnetic field enhancement in systems that contain many fluorophores in a defined geometry. In figure 16 we show preliminary results obtained for a mixture of PCP complexes and Ag nanowires. Silver nanowires were synthesized using the polyol process [67]. In a typical synthesis 3 ml ethylene glycol solution of 0.1 M silver nitrate and 3 ml of ethylene glycol solution of 0.6 M poly (vinyl pyrrolidone) (mol. wt. 55 000) were injected simultaneously into 5 ml ethylene glycol refluxed at 160 °C at a rate of 0.3 ml min^{-1}. The reaction was continuously stirred using a magnetic stirrer and the reaction mixture was refluxed at 160 °C for 60 min. After cooling, the reaction mixture was diluted with acetone and centrifuged at 2000 rpm for 20 min to separate nanowires from particles. The nanowires have an average diameter of 60 ± 10 nm, which is much better defined than the islands in the SIF, with variations of less than 20%. The reflection image (figure 16(a)) shows the positions of the nanowires in the sample. Importantly, the concentration of the nanowires is low enough to observe every nanowire independently. The complementary image displaying fluorescence of single PCP complexes is shown in figure 16(b). Although PCP complexes are distributed on the cover slip approximately uniformly, the fluorescence originates predominantly from those located in the vicinity of the nanowires. Moreover, we observe that the fluorescence intensity of PCP complexes placed at the ends of the nanowires is stronger than of these located along the wire. Future experiments will aim at a more quantitative analysis of these results, but it is already quite obvious that, by tailoring the parameters of metal nanostructures, it is possible to control the plasmon interactions and therefore the strength of fluorescence enhancement.

7. Carbon nanotubes

Carbon nanotubes are molecular-scale tubes made of graphene sheets with outstanding properties [68]. Depending on the chirality they could be either metallic or semiconducting, which by itself offers an excellent way to tune the electric and optical properties of these nanostructures. They are also one of the stiffest and strongest fibers known. These unique characteristics place carbon nanotubes as one of the most promising candidates for applications based on nanotechnology and nanostructures. Remarkably, due to the

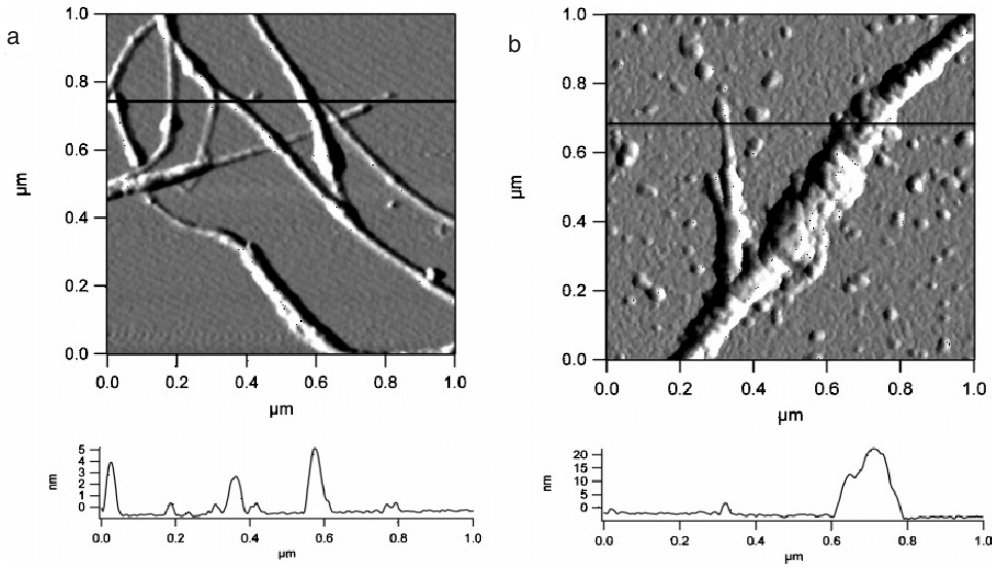

Figure 17. Atomic force microscopy images together with section curves of (a) single-walled nanotubes and (b) the photosynthetic reaction centers sitting on single-walled carbon nanotube. Original scan size is 1 μm for the SWNTs and for the SWNT/RC complex. The average height of the RC, SWNT and SWNT/RC complex is 9 ± 1 nm, 1–4 nm and 15 ± 2 nm, respectively. (Reprinted with permission from [69]. Copyright 2006 American Chemical Society.)

large active surface of the nanotubes, they can be considered as possible candidates for bridging fragile biomolecules, such as light-harvesting systems, with electric circuits. The first step towards this direction is to connect the two components in a controlled and robust way.

Recently, first attempts have been made to fabricate a hybrid nanostructure composed of a carbon nanotube and photosynthetic [69, 70]. It was shown that reaction centers from the purple bacteria can be attached to single-walled carbon nanotubes with non-specific van der Waals interaction. The binding can be seen using atomic force microscopy measurement, as shown in figure 17. Pure nanotubes feature diameters between 1 and 4 nm (figure 17(a)), while upon binding of reaction centers (figure 17(b)) the thickness increases by an average of 10 nm. This increase corresponds to the size of the reaction center (∼9 nm). The data suggest strongly that there is an effective binding of reaction centers to single-walled carbon nanotubes. The attachment of photosynthetic complexes to carbon nanotubes leads to modification of electronic properties of such hybrid nanostructures, as observed using absorption spectroscopy [69]. More controlled bridging of these two types of nanostructures has been achieved through robust covalent bonding [70]. In this case carboxyl groups were attached to carbon nanotubes, while the protein of Photosystem I was modified by attaching two cysteine groups on one side of the protein. Such a procedure enabled us to conjugate nanotubes with photosystem I. Absorption spectra of these hybrid nanostructures features contributions attributable to carbon nanotubes alongside the ones originating from the photosynthetic protein. The ability to covalently bind these two nanostructures is an important step towards using such a hybrid in nanoscale photovoltaic and optoelectronic devices.

8. Summary and outlook

The research aimed at bridging photosynthetic complexes with inorganic nanostructures has started about five years ago, yet several important observations have been demonstrated. Of the most significant are plasmon-enhanced absorption and emission of light-harvesting complexes, tunability of the energy transfer due to plasmon coupling, conjugation of photosystems with carbon nanotubes as well as metal and semiconductor surfaces. In the case of hybrid nanostructures involving carbon nanotubes photoresponse due to electron transfer has been obtained. These are stepping stones towards understanding and designing hybrid nanostructures involving natural biological systems. We anticipate at least two major directions these studies would be continuing in the coming years. First of all, huge progress can be made in controlling the optical properties of light-harvesting systems using plasmon engineering. With proper design of metallic nanoparticles and thus tuning of the plasmon resonances, the interactions can be directed into particular absorption and emission bands of a given light-harvesting complex. While spherical nanoparticles feature only one plasmon resonance, metallic nanorods are characterized with two resonances, each associated with one direction (parallel or perpendicular to the axis of a nanorod). In particular, in the case of the PCP complex, the plasmon resonances tuned to Per absorption and Chl absorption would lead to optimization of the absorption of light by these two pigments. Second, since plasmon excitation and its influence upon the optical properties of pigments depends on the distance it is important to determine optimal geometry in this regard. One way to control the separation would be bioconjugation of previously functionalized components. In this case, in order to effectively change the distance, a linker with tunable length is required, such as DNA. Another approach could be based on an SiO_2 separating layer. It can be fabricated via

chemical synthesis of metal nanoparticles or semiconductor nanocrystals with a thin silica shell, or by evaporating an SiO_2 layer using electron beam evaporation. We note that the second approach opens a way to fabricate large-area structures, which could be potentially more appealing for applications. It stems from sub-nanometer resolution of the electron beam evaporation technique. Still, the challenges remain to attach light-harvesting complexes in the same way to the surface. Only that ensures that the great advantage of electron beam evaporation can be fully exploited. On the other hand, semiconductor nanocrystals with their huge absorption coefficients and tunable ground state energies are excellent candidates to enhance and broaden the spectral range utilized by natural light-harvesting complexes. In this case the critical question concerns adjustment of the energy transfer between the nanocrystals and the pigments. Again, since the distance between donor and acceptor is one of the vital parameters determining the efficiency of the energy transfer, it would be required to control the separation with sub-nanometer accuracy. Actually, similar methods as in the case of plasmonic nanostructures could be adopted. Also, in close analogy with metallic nanoparticles, spectral properties of two components comprising a hybrid system should be carefully considered. The flexibility of chemical synthesis, which enables fabrication of homogeneous nanocrystals with well-defined absorption and emission properties, would be of considerable advantage along with the ability to functionalize the surface with various groups for possible bioconjugation.

From the point of view of biochemical manipulation of light-harvesting and photosynthetic complexes we underline the importance of modifying the pigment composition in these protein complexes and attaching active groups to the protein to enable bioconjugation. In many cases the native systems contain no active groups that could be utilized for conjugating the complex with other nanostructures, it is required to genetically modify them. On the other hand, the ability to change pigments provides yet another degree of freedom in matching spectral properties of nanostructures constituting a hybrid system.

In summary, interdisciplinary effort is necessary in developing approaches to combine biological systems with inorganic nanostructures for increased harvesting of sunlight energy and converting it into some usable form. Semiconductor and metallic nanoparticles as well as carbon nanotubes together with almost infinite ways to tune their properties provide a unique ensemble for exploring interactions in newly designed hybrid nanostructures.

Acknowledgments

Financial support from the WELCOME program 'Hybrid nanostructures as a stepping-stone towards efficient artificial photosynthesis' awarded by the Foundation for Polish Science is gratefully acknowledged. I thank Marc Brecht, Wolfgang Heiss and John M Kelly for providing unpublished data and information used in this work, as well as Christoph Braeuchle (LMU Munich), Alexander Govorov (Ohio University, Athens), Achim Hartschuh (LMU Munich), Eckhard Hofmann (University of Bochum), Nicholas Kotov (University of Michigan), Hugo Scheer (LMU Munich) and the members of their research groups involved in parts of this study.

References

[1] Cogdell R J and Lindsay J G 1998 *Tibtech* **16** 521
[2] Kodis G, Terazono Y, Liddell P A, Andreasson J, Garg V, Hambourger M, Moore T A, Moore A L and Gust D 2006 *J. Am. Chem. Soc.* **128** 1818
[3] Rodrguez-Morgade M S, Plonska-Brzezinska M E, Athans A J, Carbonell E, de Miguel G, Guldi D M, Echegoyen L and Torres T 2009 *J. Am. Chem. Soc.* **131** 10484
[4] Frolov L, Rosenwaks Y, Carmeli C and Carmeli I 2005 *Adv. Mater.* **17** 2434
[5] Mackowski S, Wörmke S, Maier A J, Brotosudarmo T H P, Harutyunyan H, Hartschuh A, Govorov A O, Scheer H and Bräuchle C 2008 *Nano Lett.* **8** 558
[6] Govindjee (ed) 1982 *Photosynthesis* (New York: Academic)
[7] Jordan P, Fromme P, Witt H T, Klukas O, Saenger W and Krauss N 2001 *Nature* **411** 909
[8] Loll B, Kern J, Saenger W, Zouni A and Biesiadka J 2005 *Nature* **438** 1040
[9] McDermot G, Prince S M, Freer A A, Howthornthwaite-Lawless A M, Papiz M Z, Cogdell R J and Isaacs N W 1995 *Nature* **374** 517
[10] Cogdell R J, Isaacs N W, Freer A A, Howard T D, Gardiner A T, Prince S M and Papiz M Z 2003 *FEBS Lett.* **555** 35
[11] Scheuring S, Sturgis J, Prima V, Bernadac A, Lévy D and Rigaud J L 2004 *Proc. Natl Acad. Sci. USA* **101** 11293
[12] Bopp M A, Jia Y W, Li L Q, Cogdell R J and Hochstrasser R M 1997 *Proc. Natl Acad. Sci. USA* **94** 10630
[13] van Oijen A M, Ketelaars M, Köhler J, Aartsma T J and Schmidt J 1999 *Science* **285** 400
[14] Hofmann E, Wrench P M, Sharples F P, Hiller R G, Welte W and Diederichs K 1996 *Science* **272** 1788
[15] Zigmatas D, Hiller R G, Sundström V and Polìvka T 2002 *Proc. Natl Acad. Sci. USA* **99** 16760
[16] Kleima F J, Hofmann E, Gobets B, Van Stokkum I H M, van Grondelle R, Diederich K and van Amerongen H 2000 *Biophys. J.* **78** 344
[17] Wörmke S, Mackowski S, Brotosudarmo T H P, Jung C, Zumbusch A, Ehrl M, Scheer H, Hofmann E, Hiller R and Bräuchle C 2007 *Biochim. Biophys. Acta–Bioenergetics* **1767** 956
[18] Brotosudarmo T H P, Hofmann E, Hiller R G, Wörmke S, Makowski S, Zumbusch A, Bräuchle C and Scheer H 2006 *FEBS Lett.* **580** 5257
[19] Polìvka T, Pascher T, Hiller R G and Sundström V 2005 *Photosyn. Res.* **86** 217
[20] Mackowski S, Wörmke S, Brotosudarmo T H P, Jung C, Hiller R G, Scheer H and Bräuchle C 2007 *Biophys. J.* **93** 3249
[21] Schulte T, Niedzwiedzki D M, Birge R R, Hiller R G, Polivka T, Hofmann E and Frank H A 2009 *Proc. Nat. Acad. Sci.* **106** 20764
[22] Leonard D, Krishnamurthy M, Reaves C M, Denbaars S P and Petroff P M 1993 *Appl. Phys. Lett.* **63** 3203
Mackowski S 2002 *Thin Solid Films* **412** 96
[23] Heinrichsdorff F, Krost A, Grundmann M, Bimberg D, Kosogov A and Werner P 1996 *Appl. Phys. Lett.* **68** 3284
[24] Peng X, Manna L, Yang W, Wickham J, Scher E, Kadavanich A and Alivisatos A P 2000 *Nature* **404** 59
[25] Murray C B, Norris D J and Bawendi M G 1993 *J. Am. Chem. Soc.* **115** 8706
[26] Rogach A, Kershaw S, Burt M, Harrison M, Kornowski A, Eychmuller A and Weller H 1999 *Adv. Mater.* **11** 552
[27] Tang Z Y and Kotov N A 2005 *Adv. Mater.* **17** 951

[28] Hines M A and Guyot-Sionnest P 1996 *J. Phys. Chem.* **100** 468
[29] Yin Y and Alivisatos A P 2005 *Nature* **437** 664
[30] Tang Z, Kotov N A and Giersig M 2002 *Science* **297** 237
[31] www.nanocluster.mit.edu
[32] Lakowicz J R 1999 *Principles of Fluorescence Spectroscopy* (New York: Kluwer Academic/Plenum)
[33] Michler P, Imamoglu A, Mason M D, Carson P J, Strouse G F and Buratto S K 2000 *Nature* **406** 968
[34] Bruchez M P, Moronne M, Gin P, Weiss S and Alivisatos A P 1998 *Science* **281** 2013
[35] Maier S A 2007 *Plasmonics. Fundamentals and Applications* (Berlin: Springer)
[36] Elghanian R, Storhoff J J, Mucic R C, Letsinger R L and Mirkin C A 1997 *Science* **277** 1078
[37] Lee J, Hernandez P, Lee J, Govorov A O and Kotov N A 2007 *Nat. Mater.* **6** 291
[38] Lakowicz J R 2006 *Plasmonics* **1** 5
[39] Dubertret B, Calame M and Liebchaber A J 2001 *Nat. Biotechnol.* **19** 365
[40] Slocik J M, Tam F, Halas N J and Naik R R 2007 *Nano Lett.* **7** 1054
[41] Anger P, Bharadwaj P and Novotny L 2006 *Phys. Rev. Lett.* **96** 113002
[42] Ray K, Badugu R and Lakowicz J R 2006 *J. Am. Chem. Soc.* **128** 8998
[43] Taminiau T H, Stefani F D, Segerink F B and van Hulst N F 2008 *Nat. Photon.* **2** 234
[44] Camden J P, Dieringer J, Zhao J and Van Duyne R P 2008 *Acc. Chem. Res.* **41** 1653
[45] Jana N R, Gearheart L and Murphy C J 2001 *J. Phys. Chem.* B **105** 4065
[46] Sun Y, Gates B, Mayers B and Xia Y 2002 *Nano Lett.* **2** 165
[47] Chen S, Wang Z L, Ballato J, Foulger S H and Carroll D L 2003 *J. Am. Chem. Soc.* **125** 16186
[48] Aherne D, Charles D E, Brennan-Fournet M E, Kelly J M and Gun'ko Y K 2009 *Langmuir* **25** 10165
[49] Aherne D, Ledwith D M, Gara M and Kelly J M 2008 *Adv. Funct. Mater.* **18** 2005
[50] Sonnichsen C, Franzl T, Wilk T, von Plessen G and Feldmann J 2002 *New J. Phys.* **4** 93.1
[51] Prodan E, Nordlander P and Halas N J 2003 *Nano Lett.* **3** 1411
[52] Flors C, Oesterling I, Schnitzler T, Fron E, Schweitzer G, Sliwa M, Herrmann A, van der Auweraer M, de Schryver F C, Mullen K and Hofkens J 2007 *J. Phys. Chem.* C **111** 4861
[53] Berera R, van Stokkum I H M, Kodis G, Keirstead A E, Pillai S, Herrero C, Palacios R E, Vengris M, van Grondelle R, Gust D, Moore T A, Moore A L and Kennis J T M 2007 *J. Phys. Chem.* B **111** 6868
[54] Mamedov A A, Belov A, Giersig M, Mamedova N N and Kotov N A 2001 *J. Am. Chem. Soc.* **123** 7738
[55] Franzl T, Klar T A, Schietinger S, Rogach A L and Feldmann J 2004 *Nano Lett.* **4** 1599
[56] Lee J, Govorov A O and Kotov N A 2005 *Nano Lett.* **5** 2063
[57] Dulkeith E, Ringler M, Klar T A, Feldmann J, Munoz Javier A and Parak W J 2005 *Nano Lett.* **5** 585
[58] Rogobete L, Kaminski F, Agio M and Sandoghdar V 2007 *Opt. Lett.* **32** 1623
Kühn S, Hakanson U, Rogobete L and Sandoghdar V 2006 *Phys. Rev. Lett.* **97** 017402
[59] Kulakovich O, Strekal N, Yaroshevich A, Maskevich S, Gaponenko S, Nabiev I, Woggon U and Artmeyev M 2002 *Nano Lett.* **2** 1449
[60] Shimizu K T, Woo W K, Fisher B R, Eisler H J and Bawendi M G 2002 *Phys. Rev. Lett.* **89** 117401
[61] Lee J, Govorov A O, Dulka J and Kotov N A 2004 *Nano Lett.* **4** 122323
[62] Roither J 2009 *PhD Thesis* University of Linz, Austria
[63] Brecht M, Radics V, Nieder J B and Bittl R 2009 *Proc. Nat. Acad. Sci.* **106** 11857
[64] Govorov A O and Carmeli I 2007 *Nano Lett.* **7** 620
[65] Wörmke S, Mackowski S, Brotosudarmo T H P, Garcia A, Braun P, Scheer H, Hofmann E and Bräuchle C 2007 *Appl. Phys. Lett.* **90** 193901
[66] Link S and El-Sayed M 1999 *J. Phys. Chem.* B **103** 8410
[67] Sun Y G and Xia Y N 2002 *Adv. Mater.* **14** 833
[68] Dresselhaus M S, Dresselhaus G and Avouris P (ed) 2000 *Carbon Nanotubes: Synthesis, Structure, Properties, and Applications* (Berlin: Springer)
[69] Dorogi M, Balint Z, Miko C, Vileno B, Milas M, Hernadi K, Forro L, Varo G and Nagy L 2006 *J. Phys. Chem.* B **110** 21473
[70] Carmeli I, Mangold M, Frolov L, Zebli B, Carmeli C, Richter S and Holleitner A W 2007 *Adv. Mater.* **19** 3901